

## Mechanisms of Target Poisoning during Magnetron Sputtering as Investigated by Real-Time *in situ* Analysis and Collisional Computer Simulation

D. Güttler, B. Abendroth, R. Grötzschel, W. Möller and D. Depla<sup>1</sup>

<sup>1</sup>Dept. Solid State Sciences, University of Ghent, Gent, Belgium

Magnetron sputtering [1-3] is one of the most frequently applied tools for the deposition of high-quality functional coatings. For high-rate deposition, sputtering of compound films is often performed in the "reactive" mode [4,5], where a metal target is exposed to a discharge in a rare gas with some fraction of reactive gas (such as oxygen or nitrogen) added. The performance of reactive sputtering is, however, impeded by the effect of target "poisoning", which means that a compound film is not only formed on the substrate as desired, but also on the sputter target, which results in a significantly reduced sputter yield and, thereby, reduced deposition rate. A further consequence of poisoning is a hysteresis of the reactive gas partial pressure at increasing/decreasing reactive gas flow, and, associated to this, an unstable operation regime between high and low target uptake at constant partial flow of the reactive gas, which often requires additional means of stabilization in practical applications [4,6]. These phenomena have been quantitatively described by a global stationary analytical model [7,8] taking into account the reactive gas balance and a saturable reactive gas chemisorption on the surface of both the target and the other surrounding surfaces including the substrate. These models have been validated semi-quantitatively (e.g., Refs. 4, 9 and 10) by comparing their predictions to experimental findings, which relate the external process parameters such as ingoing flow and partial pressure of the reactive gas to the film deposition rate and stoichiometry. Recently, it has been proposed that, in addition to surface adsorption, ion implantation affects the target uptake [11]. This has also been studied by collisional computer simulation in dynamic mode [12] using the TRIDYN [13,14] code. So far, however, no direct experimental evidence has been given on the presence and the amount of the reactive gas uptake in the target during the reactive sputtering process. Even *ex situ* measurements after deposition [15] would not allow for unambiguous conclusions, as at least a fraction of the uptake might have transient character, as, e.g., due to diffusion and/or desorption. A further complication arises from the

laterally inhomogeneous plasma-surface interaction at the target, which is due to the toroidal shape of a magnetron plasma, and the corresponding formation of the erosion "race track". Therefore, an experiment has been designed which allows for real-time *in situ* analysis of the reactive element uptake at the target surface, with the aims (i) to perform for the first time quantitative measurements of the reactive gas uptake in the target during the sputtering process and at varying lateral positions on the surface, (ii) to demonstrate the predicted hysteresis effect also for the target uptake, and (iii) to identify any transients of the target uptake after switching off the plasma.

A standard magnetron sputter configuration was installed in an ultrahigh vacuum chamber attached to the beam line system of a 5 MV tandem ion accelerator. A planar circular DC magnetron of 2" diameter was equipped with a 99.995% purity titanium target and positioned in front of a grounded stainless steel substrate plate at a distance of 10 cm. Due to differential pumping, a beam line pressure of  $< 10^{-6}$  mbar was maintained at an operating pressure around  $3 \times 10^{-3}$  mbar in the processing chamber. A fixed argon flow of 10.4 sccm and a variable nitrogen flow up to 2 sccm were admitted using flow controllers. The partial pressures of the gases were measured by means of a quadrupole mass spectrometer, which was calibrated in pure Ar and N<sub>2</sub>, respectively. The magnetron was operated in constant current mode at  $I = 0.3$  A, resulting in a target voltage around 340 V. The analysing beam of 1.8 MeV D<sup>+</sup> ions with a typical current of 40 nA was directed onto the target surface through a small hole in the substrate plate. The size of the beam spot was  $1.5 \times 2$  mm<sup>2</sup>. A tilt mechanism at the magnetron suspension allows for the analysis of different radial positions on the target surface. The  $\alpha$  particle yields from the  $^{14}\text{N}(d,\alpha_0)^{12}\text{C}$  and  $^{14}\text{N}(d,\alpha_1)^{12}\text{C}^*$  nuclear reactions were measured by means of a surface barrier detector behind a second hole in the substrate plate. The detector was covered by a thin metal foil in order to prevent any contact with the plasma. In addition, a moveable holder with additional exchangeable foils was

installed between the substrate plate and the detector to prevent the latter from film deposition which would cause an excessive energy loss of the emitted  $\alpha$  particles. Due to the high  $Q$  value of the employed nuclear reaction, background-free energy spectra are obtained at  $\sim 9$  and  $\sim 6$  MeV for the  $\alpha_0$  and  $\alpha_1$  reaction channels. The integral yield of the peaks is proportional to the areal density of nitrogen in the target surface. The calibration of the areal density was performed by means of a Ti sample implanted with  $(1 \pm 0.02) \times 10^{17} \text{ N}^+/\text{cm}^2$  at 150 keV resulting in a mean depth of 200 nm. By time-dependent analysis of the nitrogen areal density with the magnetron switched off, it was assured that there is no release of nitrogen induced by the analysing ion beam. Due to the low cross section of the nuclear reaction, the convenience of the present experiment is hampered by long analysis times of 30 min and more, which still yield no more than about 100 counts of the  $\alpha$  spectra. This, however, does not deteriorate other than the statistical quality of the results as all measurements have been performed in stationary state.

Figure 1(a) displays the evolution of the nitrogen uptake in the centre of the race track at varying nitrogen gas flow, as obtained during magnetron sputtering. (The variation of the nitrogen uptake across the entire area of the target is less than about  $\pm 50\%$ .) As in the evolution of the nitrogen partial pressure (Fig. 1(b)), the expected transition from metallic to poisoned mode at low and high nitrogen flow, respectively, is observed, being accompanied by the hysteresis effect. Whereas the partial pressure data are in qualitative agreement with findings described in literature (e.g., Ref. 16), the dynamic reactive gas uptake is measured for the first time during magnetron processing. The results are qualitatively consistent with earlier predictions by analytical modelling [7,8]. However, the absolute nitrogen content at high nitrogen flow significantly exceeds the areal density of one adsorbed monolayer, which indicates that other mechanism than surface adsorption only govern the nitrogen uptake. This will be further discussed below.

When comparing the target nitrogen content during magnetron operation and after switching off the magnetron, no nitrogen loss was observed within the experimental errors in any of the experiments. This is also shown in Fig. 1 for selected data. This indicates the absence of a significant mobile fraction of incorporated nitrogen in addition to the chemically bound one, and is in contrast to the interpretation of target voltage measurements after switching off the magnetron [17], which, however, were performed for the reactive sputtering of compounds other than TiN.

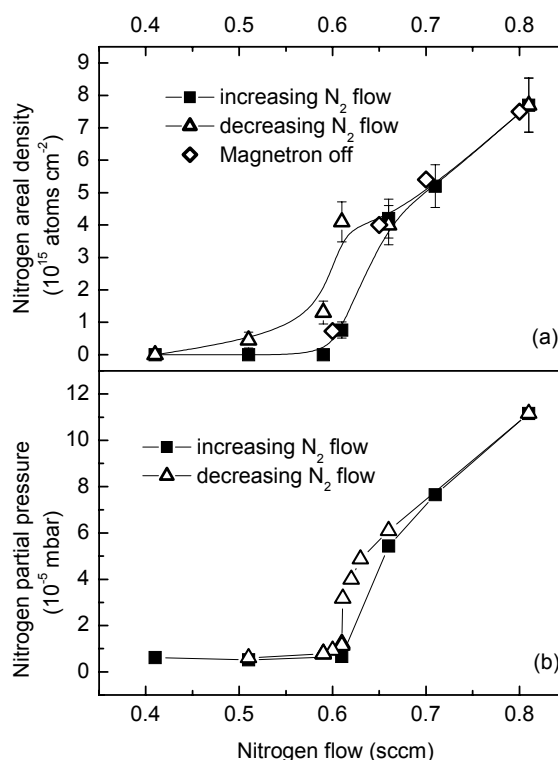


**Fig. 1:** Nitrogen uptake of the target surface (a) and nitrogen gas partial pressure (b) during sputter magnetron operation, at increasing (full squares) and decreasing (open triangles) nitrogen flow. The argon gas flow was 10.4 sccm. Location of the analysis is the centre of the race track. The diamonds denote the respective nitrogen uptake after switching off the magnetron.

Figure 2 shows the nitrogen partial pressure during operation and the target uptake measured after switching off the magnetron. At increasing nitrogen flow, the target uptake saturates around  $1.05 \times 10^{16} \text{ N}/\text{cm}^2$ . Again, this number clearly exceeds one adsorbed monolayer. This contradiction to earlier models [7,8] can be explained by ion implantation of reactive ions into the target surface. In order to quantify this effect, dynamic collisional computer simulations have been performed using the TRIDYN [13,14] program for different ratios of the nitrogen and argon partial pressures. Due to similar electron impact ionisation cross sections for Ar and  $\text{N}_2$  [18], the relative yields of  $\text{Ar}^+$  and  $\text{N}_2^+$  ions from an Ar/ $\text{N}_2$  low-temperature plasma are roughly equal to the relative partial pressures.  $\text{Ar}^+$  ions enter the target surface with the full energy  $eU_T$ , with  $e$  denoting the elementary charge and  $U_T$  the target voltage (the small addition due to the plasma potential is neglected). In contrast, for each  $\text{N}_2^+$  ion two energetic nitrogen atoms enter at  $eU_T/2$ . Additionally, 0.25  $\text{N}^+$  ions impinge on the surface at full energy per each incident  $\text{N}_2^+$  ion, which is typical for this kind of discharges, see, e.g., Refs. 19 and 20. From the target current, the laterally averaged total ion flux can be estimated to about

$1 \times 10^{17} \text{ cm}^{-2} \text{ s}^{-1}$ , as secondary electron emission is small [21]. Furthermore, there are two possible sources of thermal nitrogen atoms available for adsorption. At an  $\text{N}_2$  admixture of 10% and a total pressure of 0.3 Pa, the neutral molecules deliver a flux of  $1.5 \times 10^{17} \text{ cm}^{-2} \text{ s}^{-1}$  nitrogen atoms to the surface, with an unknown sticking coefficient. Alternatively, atomic nitrogen originates from the electron-induced dissociation in the plasma. The corresponding surface flux is expected to be significantly smaller than from the molecules, but difficult to quantify. Therefore, three series of calculations have been performed, (i) with the neutral nitrogen flux neglected, (ii) with the neutral nitrogen flux given by the reactive gas molecules at unity sticking, and (iii) with an  $\text{N}^0/\text{N}_2^+$  ratio of 2. The latter choice is in correspondence to the cross sections for electron impact ionisation and dissociation of  $\text{N}_2$  [22], and in rough agreement with the  $\text{N}^0/\text{N}_2^+$  density ratio in the plasma, which is given in Ref. 20 for an Ar/ $\text{N}_2$  plasma at an, however, tenfold higher total pressure. In this way, the composition of the incident flux is defined for a varying partial pressure ratio. Any uptake of Ar ions is neglected. The bulk concentration of nitrogen is limited to stoichiometric TiN, with excess nitrogen being modelled to be reemitted into the vacuum by infinitely fast diffusion. An initial target depth spacing of 0.25 nm is chosen, which corresponds to about one monolayer of Ti in the virgin state, so that the limitation of the nitrogen concentration at the surface corresponds to a saturable adsorption at about one monolayer. The surface binding energies of nitrogen and titanium, which determine the sputtering yields critically, are varied with the surface composition according to a formalism described in Ref. 23, which balances the surface binding energies with the sublimation energy of Ti, the molecular binding energy of nitrogen, and the formation energy of the TiN compound. The results of the computer simulation are shown in Fig. 2. Reasonable agreement with the experimental data is achieved when both implantation of energetic ions and surface adsorption of thermal nitrogen atoms are included, with an  $\text{N}^0/\text{N}_2^+$  ratio of 2. In contrast, the experimental data cannot be reproduced by simulations with energetic ions only. On the other hand, assuming the full flux of reactive gas to the surface being available for reaction overestimates the nitrogen uptake at low nitrogen flux considerably. The saturated nitrogen content at high nitrogen flow corresponds to a TiN layer of 2.5 nm thickness. The  $\sim 10\%$  deviation from the experimental data is consistent with the uncertainty of ion ranges in compounds.

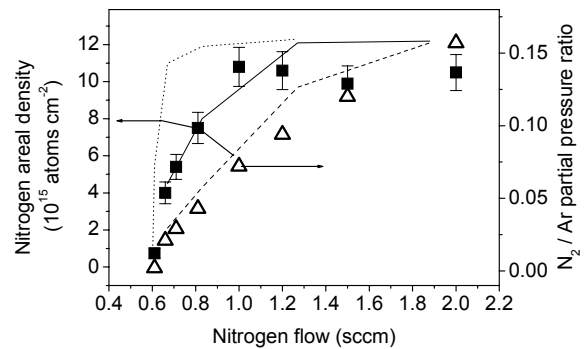


**Fig. 2:** Nitrogen-to-argon partial pressure ratio (right scale, open triangles) and nitrogen areal density at the target surface (left scale, full squares) at increasing reactive gas flow, as obtained after switching off the magnetron. Location of analysis is the center of the racetrack. The nitrogen areal density has also been calculated by TRIDYN computer simulation, with different  $\text{N}_2/\text{Ar}$  partial pressure ratios, with the relation between reactive gas flow and partial pressure ratio as given by the experimental data, and for nitrogen ion implantation and full sticking of the nitrogen molecules corresponding to an atomic nitrogen flux with  $\text{N}^0/\text{N}_2^+ = 15$  (dotted line), nitrogen ion implantation and an atomic nitrogen flux with  $\text{N}^0/\text{N}_2^+ = 2$  (solid line), and nitrogen ion implantation only (dashed line). At high  $\text{N}_2/\text{Ar}$  partial pressure ratio, the calculated areal density corresponds to 2.5 nm of stoichiometric TiN.

The collisional computer simulation describes the stationary nitrogen depth profiles as resulting primarily from the adsorption and recoil implantation of thermal nitrogen atoms, ion implantation of energetic ions, and sputtering. The comparison to the experimental results suggests that both ion implantation and surface adsorption are effective. The significance of ion implantation is basically consistent with the recent suggestion by Depla *et al.* [11] that ion implantation has to be taken into account for the description of plasma-target interaction during magnetron sputtering, and with very recent analytical modelling of the reactive sputtering kinetics taking into account ion implantation [12]. In addition, the satisfactory fit with the intermediate  $\text{N}^0/\text{N}_2^+$  flux ratio of 2 might indicate that mainly  $\text{N}^0$  constitutes the adsorbed nitrogen flux, rather than  $\text{N}_2$ . This, however, would have to be further corroborated by an improved knowledge about the individual fluxes and sticking coefficients.

The integrated content of nitrogen in the target surface amounts to roughly  $10^{17}$  atoms. At the given pressure and a nitrogen relative partial pressure of 10%, the number of nitrogen atoms in the gas volume of a 5 liter reactor amounts to about  $10^{17}$  as well. Compared to earlier understanding with an adsorbed monolayer only, this ratio of the target and gas nitrogen inventories is largely enhanced. With respect to practical applications,

this might be of importance in particular for the understanding of transient phenomena.

In summary, a deeper understanding on the plasma-target interaction during reactive magnetron sputtering has been achieved by means of real-time *in situ* target analysis and collisional computer simulation. The stationary uptake of nitrogen in a titanium target, which is laterally non-uniform across the target, results from a balance of nitrogen surface adsorption, nitrogen ion implantation, and sputtering caused by nitrogen and argon ions. There is no evidence of a mobile fraction of nitrogen which would be released after switching off the plasma.

### Acknowledgements

The authors are indebted to R. de Gryse and S. Berg for helpful comments and critical discussions, and A. Rogozin and M. Mäder for assistance in setting up the experiment and ion beam analysis, respectively.

The present results have been previously published as D. Güttler *et al.*, Appl. Phys. Lett. **85** (2004) 6134.

### References

- [1] R.F. Bunshah, Handbook of Deposition Technologies for Films and Coatings, Noyes Publ., Park Ridge, 1984.
- [2] P.Eh. Hovsepian, D.B. Lewis, W.-D. Münz, Surf. Coat. Technol. **133** (2000) 166
- [3] J.M. Schneider, S. Rhode, W.D. Sproul, A. Matthews, J. Phys. D **33** (2000) R173
- [4] I. Safi, Surf. Coat. Technol. **127** (2000) 203
- [5] A.A. Voevodin, P. Stevenson, C. Rebholz, J.M. Schneider, A. Matthews, Vacuum **46** (1995) 723
- [6] T. Wallendorf, S. Marke, C. May, J. Strümpfel, Surf. Coat. Technol. **174-175** (2003) 222
- [7] S. Berg, H-O. Blom, T. Larsson, C. Nender, J. Vac. Sci. Technol. A **5** (1987) 202
- [8] T. Larsson, H-O. Blom, C. Nender, S. Berg, J. Vac. Sci. Technol. A **6** (1988) 1832
- [9] E. Kusano, J. Appl. Phys. **70** (1991) 7089
- [10] R. Mientus, K. Ellmer, Surf. Coat. Technol. **116** (1999) 1093
- [11] D. Depla, R. De Gryse, Surf. Coat. Technol. **183** (2004) 184; **183** (2004) 190; **183** (2004) 196
- [12] O. Kappertz, D. Rosen, T. Nyberg, I. Kataradjiev, S. Berg, Int. Conf. on Metallurgical Coatings and Thin Films, San Diego, California, USA, 2004
- [13] W. Möller, W. Eckstein, Nucl. Instr. Meth. B **2** (1984) 814
- [14] W. Möller, W. Eckstein, J.P. Biersack, Comp. Phys. Comm. **51** (1988) 355
- [15] L. Combadiere, J. Machet, Surf. Coat. Technol. **82** (1996) 145
- [16] A.F. Hmiel, J. Vac. Sci. Technol. A **3** (1985) 592
- [17] D. Depla, R. De Gryse, Vacuum **69** (2003) 529
- [18] H.S.W. Massey, E.H.S. Burhop, Electronic and Ionic Impact Phenomena, Oxford University Press, London, 1956
- [19] J. Neidhardt, L. Hultman, B. Abendroth, R. Gago, W. Möller, J. Appl. Phys. **94** (2003) 7059
- [20] F. Debal, J. Bretagne, M. Jumet, M. Wautelet, J.P. Dauchot, M Hecq, Plasma Sources Sci. Technol. **7** (1998) 219
- [21] M.A. Lewis, D.A. Glocker, J. Jorne, J. Vac. Sci. Technol. A **7** (1989) 1019
- [22] Y. Itikawa, M. Hayashi, A. Ichimura, K. Onda, K. Sakimoto, K. Takayanagi, M. Nakamura, H. Nishimura, T. Takayanagi, J. Phys. Chem. Ref. Data **15** (1986) 985
- [23] W. Möller, M. Posselt, TRIDYN\_FZR User Manual, Report FZR-317, Forschungszentrum Rossendorf, 2001